Neurons differentiate magnitude and location of mechanical stimuli

Benjamin M. Gaub[a,1,2], Krishna Chaitanya Kasuba[a,1], Emilie Mace[b], Tobias Strittmatter[a], Pawel R. Laskowski[a], Sydney A. Geissler[a], Andreas Hierlemann[a], Martin Fussenegger[a], Botond Roska[b], and Daniel J. Müller[a,2]

[a]Department of Biosystems Science and Engineering, Eidgenössische Technische Hochschule Zurich, 4058 Basel, Switzerland; and [b]Neural Circuit Laboratories, Friedrich Miescher Institute for Biomedical Research, 4058 Basel, Switzerland

Edited by Bianxiao Cui, Stanford University, Stanford, CA, and accepted by Editorial Board Member Chad A. Mirkin November 27, 2019 (received for review June 12, 2019)

Neuronal activity can be modulated by mechanical stimuli. To study this phenomenon quantitatively, we mechanically stimulated rat cortical neurons by shear stress and local indentation. Neurons show 2 distinct responses, classified as transient and sustained. Transient responses display fast kinetics, similar to spontaneous neuronal activity, whereas sustained responses last several minutes before returning to baseline. Local soma stimulations with micrometer-sized beads evoke transient responses at low forces of ∼220 nN and pressures of ∼5.6 kPa and sustained responses at higher forces of ∼360 nN and pressures of ∼9.2 kPa. Among the neuronal compartments, axons are highly susceptible to mechanical stimulation and predominantly show sustained responses, whereas the less susceptible dendrites predominantly respond transiently. Chemical perturbation experiments suggest that mechanically evoked responses require the influx of extracellular calcium through ion channels. We propose that subtraumatic forces/pressures applied to neurons evoke neuronal responses via nonspecific gating of ion channels.

atomic force microscopy | calcium response | mechanobiology | mechanosensitivity | cortex neurons

It has been shown that neuronal membranes and membrane channels can be modulated by mechanical stimuli, which affect neuronal activity (1, 2). Whereas a wide body of literature describes the function of mechanosensitive membrane proteins in sensory neurons, including Piezo receptors in touch-sensitive neurons and transmembrane channel-like receptors in auditory hair cells (3), studies describing the endogenous mechanosensitivity of neurons of the central nervous system are sparse (1). Mechanosensitivity can be described as the complex interplay between proteins that enable cells to sense, transduce, and respond to mechanical stimuli and properties of their environment (4). Little is known about the force and pressure regimes in which neurons respond to mechanical stimuli. Excessive accelerating or stretching forces (5, 6), experienced during a collision in contact sports, for example, can cause failure of neuronal membranes (mechanoporation), which ultimately leads to neuronal injury and apoptosis (7). However, the effects that subtraumatic forces and pressures exert on neuronal activity remain to be described.

While it is known that axons are particularly vulnerable to mechanical insults leading to apoptosis, there is no information on whether and how the morphologically and functionally diverse neuronal compartments composing the cell body (soma), axons, and dendrites sense and respond to subtraumatic forces (8). This information is particularly important for understanding the mechanobiology of neurons and, in the near future, to engineer mechanosensitive systems for neuronal control.

Pyramidal neurons of the cortex and hippocampus can respond to mechanical forces (9). Therefore, it is conceivable that mechanical stimuli can be tailored to modulate neuronal activity. Focused ultrasound has gained attention for noninvasively stimulating deep brain areas with millimeter precision in mice (10) and humans (11, 12). This approach is thought to rely on the intrinsic mechanosensitivity of neurons, as it does not require the expression of exogenous proteins. However, the mechanisms by which focused ultrasound evokes neuronal responses, and the identity of membrane receptors that are sensitive to such stimulation, remain controversial (13, 14).

Recently, an acoustically driven piston-based device was introduced to screen mammalian cells for their ability to sense and respond to shear stress (15). So far, the assay, which has identified novel mechanosensitive membrane receptors, has not been applied to characterize neuronal systems. While the assay is well suited to simultaneously stimulate a large number of cells, it cannot apply mechanical stimuli at a precisely controllable magnitude, duration, or subcellular location. In contrast, atomic force microscopy (AFM) is a well-established tool for applying mechanical stimuli at cellular and subcellular levels (16, 17). AFM can be used to sense and apply mechanical forces at nanometer spatial resolution and picoNewton force sensitivity; for example, AFM has been used to probe the elastic moduli of neuronal compartments (18), the role of mechanical cues in axon guidance (19, 20), and the force generation by cells against extracellular confinements (21–23).

Here we mechanically stimulate entire neurons, in ensemble by shear stress, as well as subcellular compartments of single neurons, by AFM-based local indentation while monitoring their

Significance

Our study provides a quantitative and morphological framework for mechanical neuromodulation. We report that mechanical stimuli at subtraumatic forces and pressures can evoke neuronal calcium responses. Cultured cortex and hippocampus neurons respond to both global and local mechanical forces and pressures delivered by shear stress and indentation, respectively, and show either short-lived or sustained responses, depending on the magnitude and location of the applied stimulus. Chemical perturbation experiments suggest that ion channel activity is modulated by forces and pressures acting on neurons. Our insights contribute to the understanding of how neurons respond to mechanical stimuli and may guide future studies to mechanically control neurons by, for example, electromagnetic forces or ultrasound.

Author contributions: B.M.G., K.C.K., E.M., T.S., P.R.L., and D.J.M. designed research; B.M.G., K.C.K., T.S., and P.R.L. performed research; B.M.G., K.C.K., E.M., T.S., P.R.L., S.A.G., A.H., M.F., B.R., and D.J.M. contributed new reagents/analytic tools; B.M.G., K.C.K., E.M., and P.R.L. analyzed data; and B.M.G., K.C.K., E.M., P.R.L., S.A.G., A.H., M.F., B.R., and D.J.M. wrote the paper.

The authors declare no competing interest.

This article is a PNAS Direct Submission. B.C. is a guest editor invited by the Editorial Board.

[1]B.M.G. and K.C.K. contributed equally to this work.

[2]To whom correspondence may be addressed. Email: benjamin.gaub@bsse.ethz.ch or daniel.mueller@bsse.ethz.ch.

This article contains supporting information online at https://www.pnas.org/lookup/suppl/doi:10.1073/pnas.1909933117/-/DCSupplemental.

First published December 27, 2019.

functional response. We find that cortical and hippocampal neurons are highly responsive to shear stress delivered by oscillating pistons. Using an AFM-based cell mechanical assay in combination with confocal and superresolution microscopy, we observe that cortical neurons respond in 2 fundamentally different ways to the magnitude and location of the mechanical force and pressure applied. Finally, chemical perturbation experiments suggest a variety of neuronal ion channels involved in this neuronal response.

Results

Cortical Neurons Respond to Mechanical Stimulation. To test whether cortical neurons respond to shear stress, we searched for ways to mechanically stimulate and read out the activity of neurons simultaneously. Inspired by a recent study (15), we engineered a device that generates a disturbed fluid motion by oscillating a 3D printed piston array (Fig. 1*A*). The piston array, housed in a casing with CO_2 and temperature control, is driven by a loudspeaker and controlled by a signal generator (*Materials and Methods*). The movement of the pistons, immersed in culture medium, delivers shear stress to the neurons cultured in transparent 96-well plates. We cultured E18 rat cortical neurons in the well plates, transduced them with the genetically encoded calcium sensor GCaMP6S using adeno-associated viruses, and monitored the morphology and the functional calcium response of neurons before, during, and after mechanical stimulation using inverted wide-field fluorescence microscopy (Fig. 1*B*).

Initially, we mechanically stimulated the cultured neurons by applying a single shear stress stimulus (60-Hz oscillation, ∼1 to 5 Pa) of 3 s duration and observed a rapid increase of the calcium signal in the majority of GCaMP6S-expressing neurons (Fig. 1*B* and Movie S1). The mechanically evoked neurons returned to baseline fluorescence levels after ∼10 s on average. Spontaneous calcium signals, occurring in the absence of mechanical stimulation, were not affected by the evoked response (Fig. 1 *C* and *H*), indicating that the stimulation was neither invasive nor damaging. Likewise, the morphology of neurons remained unchanged after stimulation. On average, mechanically evoked calcium signals were stronger (2.9 ± 0.1 $\Delta I/I$; mean ± SEM) compared with spontaneously occurring calcium signals (2.0 ± 0.1 $\Delta I/I$) (Fig. 1*D*). By systematically analyzing ∼3,000 neurons from 21 independent experiments (*Materials and Methods*), we found that individual neurons showed 2 classes of mechanically evoked responses. The majority of neurons (n = 2,562 cells or 89%) displayed short-lived transient responses with a fast signal decay (τ = 2.5 ± 0.2 s) (Fig. 1*E*), while a small subset of neurons (n = 154 cells or 6%) showed a long-lived sustained response with a slow signal decay (τ = 4.4 ± 0.7 s) (Fig. 1*F*). The remaining 5% of GCaMP6S-expressing neurons showed no response (Fig. 1*G*). Notably, repeated mechanical stimulation of neurons by shear stress (9 rounds of stimulation at 60 Hz, 3-s duration, with a 57-s rest between stimuli) evoked reproducible responses without any significant signal attenuation (Fig. 1*H*).

We next asked whether the neuronal response to shear stress depends on the neuronal cell type and used our piston-based assay to record mechanically evoked calcium responses in hippocampal neurons transfected with GCaMP6S (*SI Appendix*, Fig. S1*A*). We

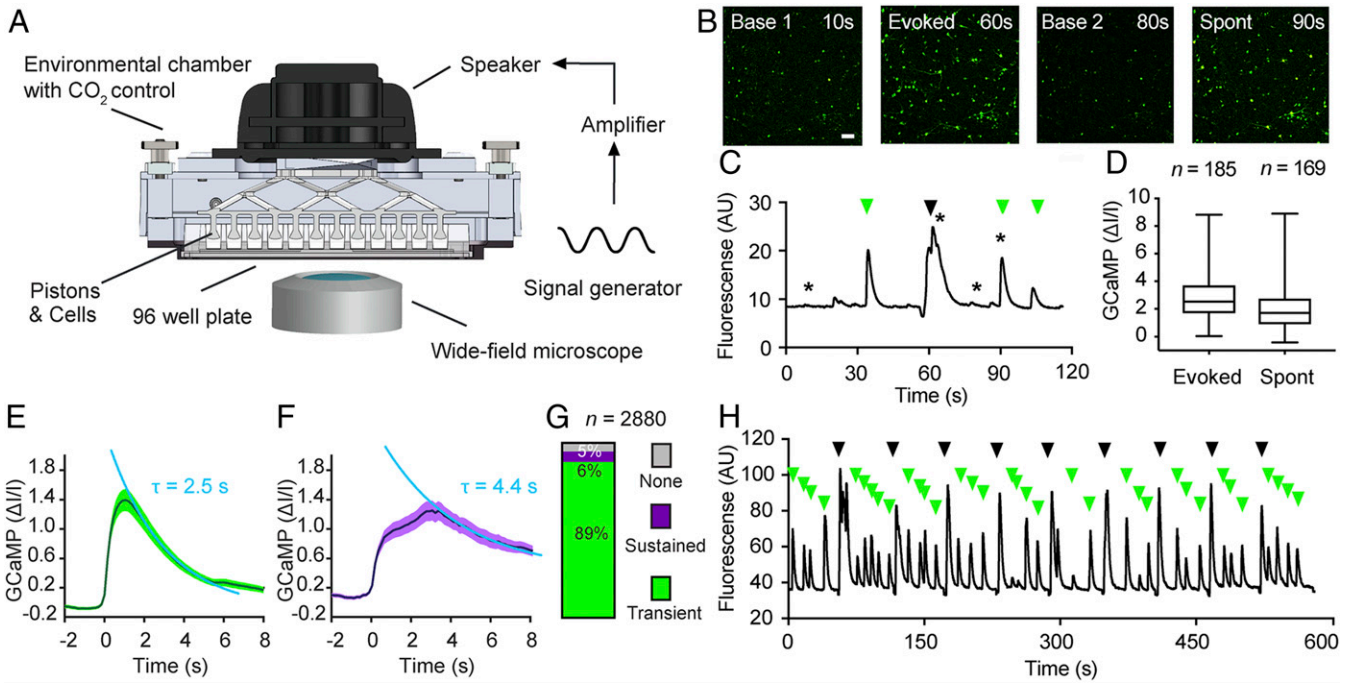

Fig. 1. Rat cortical neurons respond to mechanical stimulation by shear stress. (*A*) Schematic setup of the piston-based array used to apply shear stress to a population of neurons. (*B*) Widefield fluorescent images of cortical neurons expressing GCaMP6S (green) showing the baseline fluorescence (*Left*), mechanically evoked response (*Center Left*), return to baseline (*Center Right*), and spontaneous response in the absence of mechanical stimulation (*Right*). Images refer to time points indicated by stars in *C*. (Scale bar: 100 μm.) (*C*) Mean GCaMP6S signal (black) for a population of cortical neurons (n = 185) showing spontaneous activity (green arrows) and responses (black arrow) to a single mechanical stimulation applied by shear stress. (*D*) Quantification of *C* showing normalized GCaMP6S values for neurons with evoked (n = 185; *Left*) and with spontaneous (n = 169; *Right*) activity. Boxes show mean, whiskers show minimum and maximum values, and n refers to the number of neurons analyzed. (*E*) Average fluorescence trace showing transient evoked GCaMP6S responses of cortex neurons (n = 2,562) with an exponential decay time constant τ of 2.5 ± 0.2 s (mean ± SEM). (*F*) Average fluorescence trace showing sustained evoked GCaMP6S responses of cortex neurons (n = 154) with τ = 4.4 ± 0.7 s. Data were fitted by a single exponential function (light blue) to obtain τ values. Dark line, mean; shaded areas, SEM. (*G*) Percentage of hippocampal neurons with sustained, transient, or no response. Height of bar and numbers indicated show percentages; n represents the number of neurons analyzed. (*H*) Mean GCaMP6S signal of cortical neurons (n = 104) repeatedly stimulated with shear stress (9 stimuli of 3-s duration with a 57-s pause between individual stimuli). The recording shows persistently evoked responses (black arrows) and spontaneous activity (green arrows).

found that hippocampal neurons also sensed shear stress and resembled cortical neurons with respect to the magnitude of response (1.9 ± 0.1 $\Delta I/I$) (*SI Appendix*, Fig. S1*B*), transient response signal decay kinetics (τ = 2.1 ± 0.1 s) (*SI Appendix*, Fig. S1*C*), and response classes (*SI Appendix*, Fig. S1*E*). In the data analyzed, all GCaMP6s-expressing cells (100%) responded to piston stimulation (60-Hz oscillation, 1 to 5 Pa, 3-s duration) (*SI Appendix*, Fig. S1*E*). A very small fraction of hippocampal neurons (<1%) responded in a sustained fashion (*SI Appendix*, Fig. S1*D*).

Taken together, these experiments show that cortical and hippocampal neurons respond to shear stress. Applying the mechanical stimulation with pistons appears to be tolerated within our stimulation parameters, as neurons display spontaneous activity and preserve their intact morphology even after repeated stimulation. While applying shear stress by oscillating pistons is well suited to stimulate and record the activity of many neurons simultaneously, the technique does not give precise readouts of forces or pressures applied at the single-cell level, and does not confine the mechanical stimulus to neuronal compartments. This limitation prompted us to explore a more quantitative and spatially controllable assay for the mechanical stimulation of neurons.

Local Indentations Evoke Sustained and Transient Responses. We next combined AFM to locally apply mechanical stimuli to single neurons at nanometer and nanoNewton precision with confocal laser scanning microscopy to monitor the neuronal activity by real-time fluorescence imaging and differential interference contrast (DIC) microscopy to characterize the neuronal morphology under cell culture conditions (Fig. 2*A*). A 5-μm-diameter bead was glued to the free end of a tipless AFM microcantilever to define the contact area of microcantilever and neuron and to locally apply nondestructive forces and pressures.

We first asked whether cortical neurons respond to local indentation of the soma (cell body). To block spontaneous activity that could mask mechanically evoked neuronal activity, we applied the glutamate receptor antagonists DNQX and AP5 (*Materials and Methods*). Neurons with moderate GCaMP expression levels were selected for stimulation (Fig. 2*B*). The GCaMP fluorescence before mechanical stimulation served as a baseline reference. We positioned the bead of the microcantilever above the soma, vertically approached the neuron, and indented the soma until the deflecting microcantilever detected a force of ~200 nN (Fig. 2 *A* and *B*). After a short contact time of ~250 ms, the bead was retracted. To quantify the neuronal response, the fluorescence signal of GCaMP6S was monitored (Fig. 2*B*). Directly following the mechanical indentation, the neuron showed a strong calcium response. DIC imaging showed that the mechanical stimulation did not affect neuron morphology. Such local stimulation of the soma resulted in a "global" calcium response throughout the neuron, as shown by a fluorescence intensity heat map (Fig. 2*C*).

We then systematically investigated the response of 641 neurons to mechanical stimulation. The soma of each neuron was repeatedly indented by increasing the forces from 100 to 400 nN in 50-nN steps. Between each indentation, we allowed the neuron to rest for ~10 to 20 s. Once a neuron responded to mechanical stimulation, the stimulus protocol was terminated, and a new cell was stimulated. In total, 45% of the neurons responded to mechanical stimulation, while 55% did not (Fig. 2*G*). The neurons responded to soma indentation in 1 of 2 ways (Fig. 2*D* and *SI Appendix*, Fig. S2 *C* and *D*), either transiently or sustained. Roughly one-quarter (24%) of all stimulated neurons showed a "transient" calcium response, which returned to baseline levels within ~10 s (Fig. 2*G* and Movie S2). The transient response showed a fast rise time (mean ± SEM, 0.7 ± 0.1 s; *SI Appendix*, Fig. S2*I*) and decayed exponentially, with a time constant of τ = 3.4 ± 0.0 s (Fig. 2*E*). Some 21% of stimulated neurons showed a "sustained" calcium response (Fig. 2*G* and Movie S3), which also

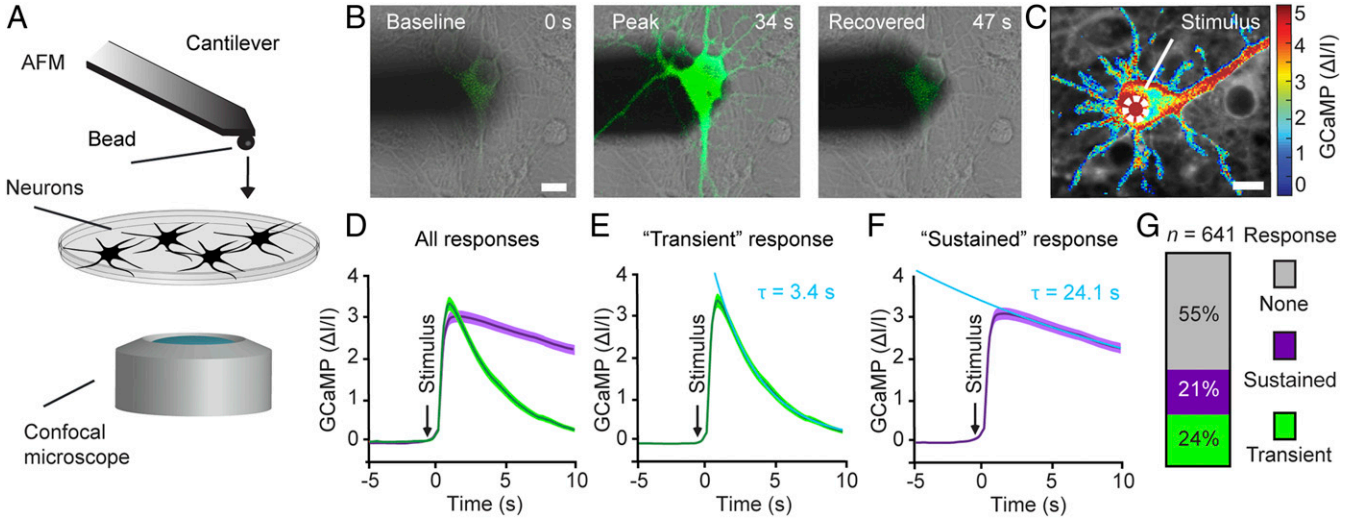

Fig. 2. Cortical neurons respond to mechanical indentation of the soma. (*A*) Schematic of the assay combining AFM with confocal microscopy. The free end of the atomic force microscope cantilever carries a bead (5 μm diameter) to indent the neuron. The neuronal response is read out via functional calcium imaging by confocal microscopy, while the cellular morphology is monitored using DIC microscopy. (*B*) Overlaid DIC and fluorescence images of an atomic force microscope cantilever (shadow) and a cortical neuron expressing GCaMP6S (green) before (*Left*), during (*Center*), and after (*Right*) mechanical stimulation. Time points are indicated in the top right corner. (*C*) Normalized fluorescence intensity heat map showing a typical calcium response of a cortical neuron to a 250-ms mechanical indentation of the soma. The white dashed circle indicates the contact area at which the cantilever bead stimulated the neuron. (*D–F*) Averaged and normalized GCaMP6S fluorescence traces of cortical neurons mechanically stimulated at the soma (dark line, mean; color shaded area, SEM). (*D*) Neuronal responses cluster into 2 groups as determined by principal component analysis (n = 143 cells). (*E*) Transient responses (green; n = 51) show an exponential decay time constant τ = 3.4 ± 0.0 s (mean ± SEM). (*F*) Sustained responses (purple; n = 92) with τ = 24.1 ± 0.2 s. Arrows indicate time points of mechanical stimulation. Data were fitted by a single exponential function (light blue) to reveal τ values. (*G*) Percentage of cortical neurons showing no, transient, or sustained response to mechanical stimulation of the soma. Height of bars and numbers both indicate percentages; n represents the number of neurons analyzed. (Scale bars: 10 μm.)

featured a fast rise time (0.8 ± 0.1 s; *SI Appendix*, Fig. S2*I*) but decayed to baseline levels within ∼100 s at an exponential time constant of τ = 24.1 ± 0.2 s (Fig. 2*F*).

We next asked whether the transient and sustained neuronal responses depend on the calcium sensor or the neuronal cell type. Thus, we recorded the mechanically evoked calcium responses of cortical neurons expressing the fast calcium sensor GCaMP6F (*SI Appendix*, Fig. S2*E*). The responses of neurons to soma stimulation clustered into transient responses, rising with $t = 0.4 \pm 0.1$ s (*SI Appendix*, Fig. S2*I*) and decaying with $\tau = 5.0 \pm 0.1$ s (*SI Appendix*, Fig. S2*E*), and sustained responses, rising with $t = 0.4 \pm 0.1$ s (*SI Appendix*, Fig. S2*I*) and decaying with $\tau = 27.9 \pm 0.9$ s (Fig. 2*F*). With respect to neuronal cell types, hippocampal neurons expressing GCaMP6S stimulated at the soma also showed similar transient responses, rising with $t = 0.5 \pm 0.0$ s (*SI Appendix*, Fig. S2*I*) and decaying with $\tau = 4.1 \pm 0.1$ s (*SI Appendix*, Fig. S2*G*), as well as sustained responses, rising with $t = 0.4 \pm 0.1$ s (*SI Appendix*, Fig. S2*I*) and decaying with $\tau = 29.2 \pm 0.5$ s (*SI Appendix*, Fig. S2*H*). These experiments suggest that the transient and sustained neuronal responses are independent of calcium sensor or neuronal cell type.

Neurons Differentiate Magnitude of Mechanical Stimuli. We next normalized the calcium response of all neurons that received soma stimulation to analyze their common features (*Materials and Methods*). The peaks of the normalized transient (2.9 ± 0.2 Δ*I*/*I*) and sustained (3.3 ± 0.2 Δ*I*/*I*) calcium response were comparable in magnitude (*SI Appendix*, Fig. S3*A*) but were broadly distributed, which may be attributed to varying levels of GCaMP expression and morphological heterogeneities. When repeatedly stimulated by stepwise increasing the indenting force, the threshold force evoking transient responses was lower than the force evoking sustained responses (mean ± SEM, 265.6 ± 5.5 nN vs. 285.5 ± 4.7 nN) (*SI Appendix*, Fig. S3*B*). The lower and higher forces correspond to lower and higher mean pressures of 6.8 ± 0.1 kPa and 7.3 ± 0.1 kPa, respectively (*SI Appendix*, Text S1). The statistically significant difference of both overlapping force distributions suggests that neurons subjected to mechanical stimuli tend to respond transiently to lower forces and pressures while they respond sustainedly to higher forces and pressures.

To further investigate the neuronal response, we changed the stimulation protocol from the ramping stimulus (applying repeated indentations of stepwise increasing force to the same neuron; see Figs. 2 and 4) to a single indentation stimulus (Fig. 3). The single indentation stimulus applied to each neuron one short indentation (∼250 ms) at either low force (pressure) of 219.5 ± 1.9 nN (5.6 ± 0.1 kPa) or high force (pressure) of 360.1 ± 1.7 nN (9.2 ± 0.0 kPa), respectively (*SI Appendix*, Text S1). Neurons indented with lower force primarily showed transient responses (60%) and fewer sustained responses (17.5%), whereas neurons indented with higher force primarily showed sustained responses (53%) and fewer transient responses (15.6%) (Fig. 3*A*). The average sustained response to higher forces and pressures showed an exponential decay (τ = 24.8 ± 0.5 s; Fig. 3*B*), closely matching the sustained response measured initially (τ = 24.1 ± 0.4 s; Fig. 2*F*), whereas the calcium signals in response to lower forces and pressures decayed much faster (τ = 9.6 ± 0.4 s; Fig. 3*B*). The fraction of neurons showing no response was similar for lower (22.5%) and higher (31.3%) forces.

We next examined whether the same neuron can show both transient and sustained responses by repeatedly stimulating the soma of single neurons while stepwise increasing the applied force (Fig. 3*C*). Indeed, the same neuron responded transiently and sustainedly to subsequent mechanical stimuli, suggesting that transient or sustained responses are not characteristic for an individual neuron. In the absence of mechanical stimulation and synaptic activity inhibitors, neurons showed spontaneous activity with similar decay times (τ = 4.4 ± 0.2 s) as observed for mechanically stimulated transient calcium responses (τ = 3.4 ± 0.0 s; Fig. 3*D*).

Taken together, these experiments demonstrate that neurons differentiate the magnitude of mechanical stimuli. At lower force, neurons tend to respond transiently, while at higher force, they respond in a sustained manner.

Neurons Differentiate the Location of Mechanical Stimuli. Having observed that local indention of the neuronal soma can induce transient or sustained responses, we asked how axons and dendrites respond to such stimulation. To identify axons in live neurons, we applied anti–pan-neurofascin antibodies, which bind the extracellular domain of neurofascin and label the axon initial segment (24). We then systematically stimulated somas, axons, and dendrites of

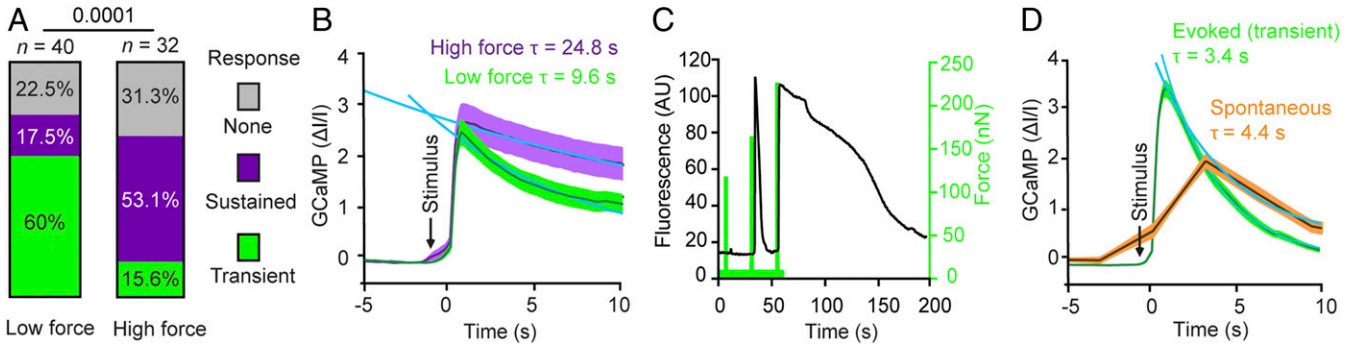

Fig. 3. Neurons differentiate the force indenting the soma. (*A* and *B*) Differential responses of cortical neurons stimulated once at low force (219.5 ± 1.9 nN; $n = 40$) or high force (360.1 ± 1.7 nN; $n = 32$). (*A*) Percentage of neurons showing no (gray), sustained (purple), or transient (green) response. The χ^2 test was used to determine statistical significance. (*B*) GCaMP6S fluorescence intensity vs. time for neurons stimulated with high force (purple) or low force (green). Dark lines represent the mean; shaded areas, the SEM. The data are fitted with single exponential functions (blue) to reveal the decay time of responses evoked at high force τ = 24.8 ± 0.5 s (mean ± SEM) and at low force τ = 9.6 ± 0.4 s. (*C*) Transient and sustained responses of the same neuron mechanically indented at the soma depends on force. GCaMP6S signal (black) for a single cortical neuron showing first no response, then a transient response, and finally a sustained response to an indentation force of ∼130 nN, ∼180 nN, and ∼240 nN (green), respectively. The duration of each mechanical stimulus was 250 ms, and a 20-s long pausing interval was applied between each stimulus. The experiment was repeated 13 times. (*D*) Comparison of transient response and spontaneous signal of cortical neurons. Shown are GCaMP6S fluorescence intensity in the absence of (spontaneous activity, orange; $n = 64$) and in response to (green; $n = 51$) mechanical stimulation. Fluorescence from transient responses taken from Fig. 2*E*. Spontaneous signals were fitted with a single exponential function (blue) revealing τ = 4.4 ± 0.2 s. Dark lines, mean; shaded error bar, SEM. *n* represents the number of neurons analyzed.

individual neurons and monitored the calcium signal (Fig. 4 and Movies S4 and S5). Mechanical stimulation of dendrites evoked "local" calcium responses in 39% of the neurons, where an increase in the GCaMP6S signal remained confined to the site of indentation. The remaining 61% of neurons showed a "global" calcium response, with increasing GCaMP6S signals propagated throughout the neuron (Fig. 4 *D* and *E*). Local responses occurred when dendrites were stimulated further away from the soma (32.1 ± 2.7 μm), whereas global responses occurred when dendrites were stimulated in closer proximity to the soma (24.6 ± 2.2 μm) (*SI Appendix*, Fig. S4*C*). In contrast, the mechanical stimulation of axons exclusively evoked global calcium responses (Fig. 4*B*). The normalized GCaMP signals were similar for mechanically stimulated axons (1.8 ± 0.2 $\Delta I/I$) and dendrites (1.8 ± 0.2 $\Delta I/I$), as were the threshold forces required to stimulate axons (230.7 ± 13.0 nN) and dendrites (232.0 ± 12.1 nN) (*SI Appendix*, Fig. S4). However, because axons are of smaller diameter than dendrites, the contact area with the indenting bead is also smaller. Thus, the resulting pressure of 42.4 ± 8.1 kPa applied to axons was higher than the 19.8 ± 1.6 kPa applied to dendrites (*SI Appendix*, Text S2).

Analysis of the different response types—transient, sustained, or none—revealed substantial differences between the neuronal compartments (Fig. 4*F*); 73% of all mechanically stimulated axons showed calcium responses, compared with 35% of dendrites and 45% of somas. Among all responding axons, 55% showed a sustained response, compared with 9% of all responding dendrites and 38% of all responding somas (Fig. 4*F*). Since more axons respond to mechanical stimulation compared with dendrites or somas, we conclude that axons are more susceptible to mechanical stimulation.

Plasma Membrane and Cytoskeleton Remain Intact. In a process known as mechanoporation, excessive stress can lead to defects in the plasma membrane (7, 8, 25, 26) through which calcium can flow along its concentration gradient into the cell. We thus wanted to test whether our mechanical stimulation assay using a beaded cantilever mechanoporates the neuronal membrane. To monitor the integrity of the cell membrane, we added the small fluorescent dye propidium iodide (PI) to the extracellular medium, mechanically stimulated the soma, and simultaneously imaged GCaMP6S (488 nm) and PI (600 nm) (*SI Appendix*, Fig. S5 *A*–*C*). While we observed strong calcium responses on mechanical indentation (3.7 ± 0.2 $\Delta I/I$), we did not observe any PI translocating into the cytosol (0.1 ± 0.0 $\Delta I/I$) of neurons (*SI Appendix*, Fig. S5 *A* and *B*). Conversely, when using cantilevers carrying a molecularly sharp conical tip that can penetrate the neuronal membrane, we found that substantial amounts of PI translocated into the cytosol (*SI Appendix*, Fig. S5*C*).

We next followed the fate of unstimulated and mechanically stimulated neurons overnight, to account for the possibility that hallmarks of injury require more time to manifest. Cortical neurons were kept under temperature- and CO_2-controlled conditions while the GCaMP and PI fluorescent signals were imaged every 10 min. Under these conditions, neurons that had not been mechanically stimulated typically survived for a mean of 350.0 ± 24.1 min before showing a strong rise in calcium levels, followed by a sudden uptake of PI, which indicated cell death (*SI Appendix*, Fig. S6*A*). Mechanically stimulating the somas had no significant effect on the survival of transiently responding (317.8 ± 9.5 min) or nonresponding (350.0 ± 57.5 min) neurons (*SI Appendix*, Fig. S6*B*). Most neurons with sustained responses fared similarly (310.0 ± 80.7 min), with 2 exceptions that loaded PI prematurely.

We further characterized the integrity of the cytoskeleton after mechanical stimulation. The axonal cytoskeleton arranges as bundles of microtubules with periodic rings of spectrin and actin (27, 28). Axons are particularly susceptible to mechanical injuries that cause microstructural trauma (7, 8). These injuries manifest in the formation of axonal beads within 60 min postinjury, followed by axonal breakdown and neuronal death. We indented the somas of cortical neurons and imaged actin rings using stimulated emission depletion (STED) microscopy at a resolution approaching 50 nm (*SI Appendix*, Fig. S7). Confocal microscopy images of the entire neuron and superresolution images of the axon showed that the neuronal morphology and the periodic actin rings along the axon remained unperturbed after mechanical stimulation of soma, axon, or dendrite. This finding was independent of whether the neurons responded to mechanical stimulation transiently or in a sustained manner. We also could not find morphological hallmarks of trauma, such as swelling or blebbing around the site of indentation, as described in earlier studies using in vitro models of traumatic brain injury (7, 25, 26, 29).

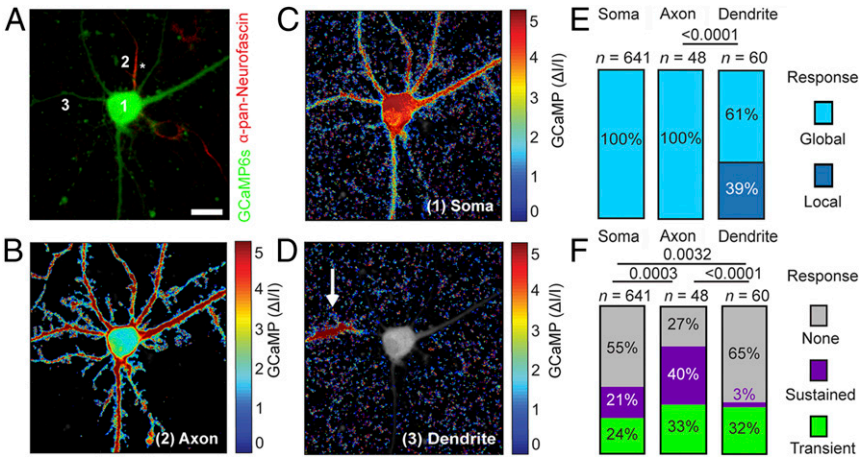

Fig. 4. Mechanical stimulation of axon, dendrite, and soma reveals differential responses. (*A*) Cortical neuron expressing GCaMP6S (green) and stained with anti–pan-neurofascin (red) to identify the axon. (*B*–*D*) Normalized fluorescence intensity heat maps showing averaged calcium responses to a 250-ms mechanical indentation of axon (*B*), soma (*C*), and dendrite (*D*). The locations of the mechanical stimuli are indicated by numbers 1–3 in *A*. Dendrite stimulation shows local calcium responses (white arrow); soma and axon stimulations show a global calcium response. The axon is marked by an asterisk. (Scale bar: 10 μm.) (*E* and *F*) Response types of cortical neurons to mechanical indentation of soma, axon, or dendrite. (*E*) Percentage of neurons showing local (dark blue) and global (light blue) responses. (*F*) Percentages of neurons showing no response (gray), sustained response (purple), and transient response (green). *n* represents the number of neurons analyzed. The χ^2 test was used for statistical analysis.

Taken together, these results suggest that the mechanical stimulation applied in this study lies outside the range of the mechanical perturbations that cause neuronal injury.

Neurons Respond via Calcium Influx through Ion Channels. To investigate the mechanism of mechanically evoked calcium responses, we applied a number of chemical compounds to our shear stress and local indentation assays and asked whether they can inhibit mechanically evoked responses. To this end, we compared the proportions of responding cortical neurons before and after the addition of each chemical compound (*Materials and Methods*). Application of vehicle alone (0.1% DMSO for piston, 1% DMSO for AFM) had no effect on the overall responses to mechanical stimulation by shear stress (Fig. 5*A*) and local indentation (*SI Appendix*, Fig. S2*A*).

To identify the source of calcium leading to the observed neuronal response, we added the cell-impermeable calcium chelator BAPTA free acid to the extracellular medium. Removal of extracellular calcium abolished mechanically evoked responses from 1.2 ± 0.1 $\Delta I/I$ to 0.0 ± 0.0 $\Delta I/I$ in piston experiments (Fig. 5*B*). Similarly, for AFM stimulation, the percentage of responsive neurons decreased from 82% to 27% (*SI Appendix*, Fig. S8*A*). Thus, in neurons responding to mechanical stimulation, extracellular calcium crosses the membrane, which elevates the intracellular GCaMP6S signal.

We next decided to chemically perturb a variety of ion channels that we considered good candidates to mediate the mechanically evoked response. All perturbed channels were abundant in cortical neurons, as shown by their mRNA transcript levels (*SI Appendix*, Table S1). Application of tetrodotoxin (TTX), a blocker of voltage-gated sodium channels, strongly suppressed the neuronal calcium responses to mechanical stimulation by shear stress, from 2.7 ± 0.1 $\Delta I/I$ to 0.2 ± 0.0 $\Delta I/I$ (Fig. 5*C*). Notably, the transient responses to local indentation by AFM decreased from 61% to 32%, while the sustained responses did not change much (31% vs. 28%) (*SI Appendix*, Fig. S8*B*). Application of benipidine, a blocker of voltage-gated calcium channels, also strongly suppressed the neuronal response to shear stress, from 2.9 ± 0.1 $\Delta I/I$ to 0.1 ± 0.0 $\Delta I/I$ (Fig. 5*D*).

We next tested whether canonical mechanosensitive channels endogenously expressed in neurons, including the transient receptor potential (TRP) (30) and Piezo1 (19) channels, give rise to the calcium signal. The addition of the peptide GsMTx4, an inhibitor of mechanosensitive cation channels (31), considerably reduced the neuronal response to mechanical stimuli by shear stress (2.5 ± 0.1 $\Delta I/I$ vs. 1.6 ± 0.1 $\Delta I/I$) (Fig. 5*E*), whereas it did

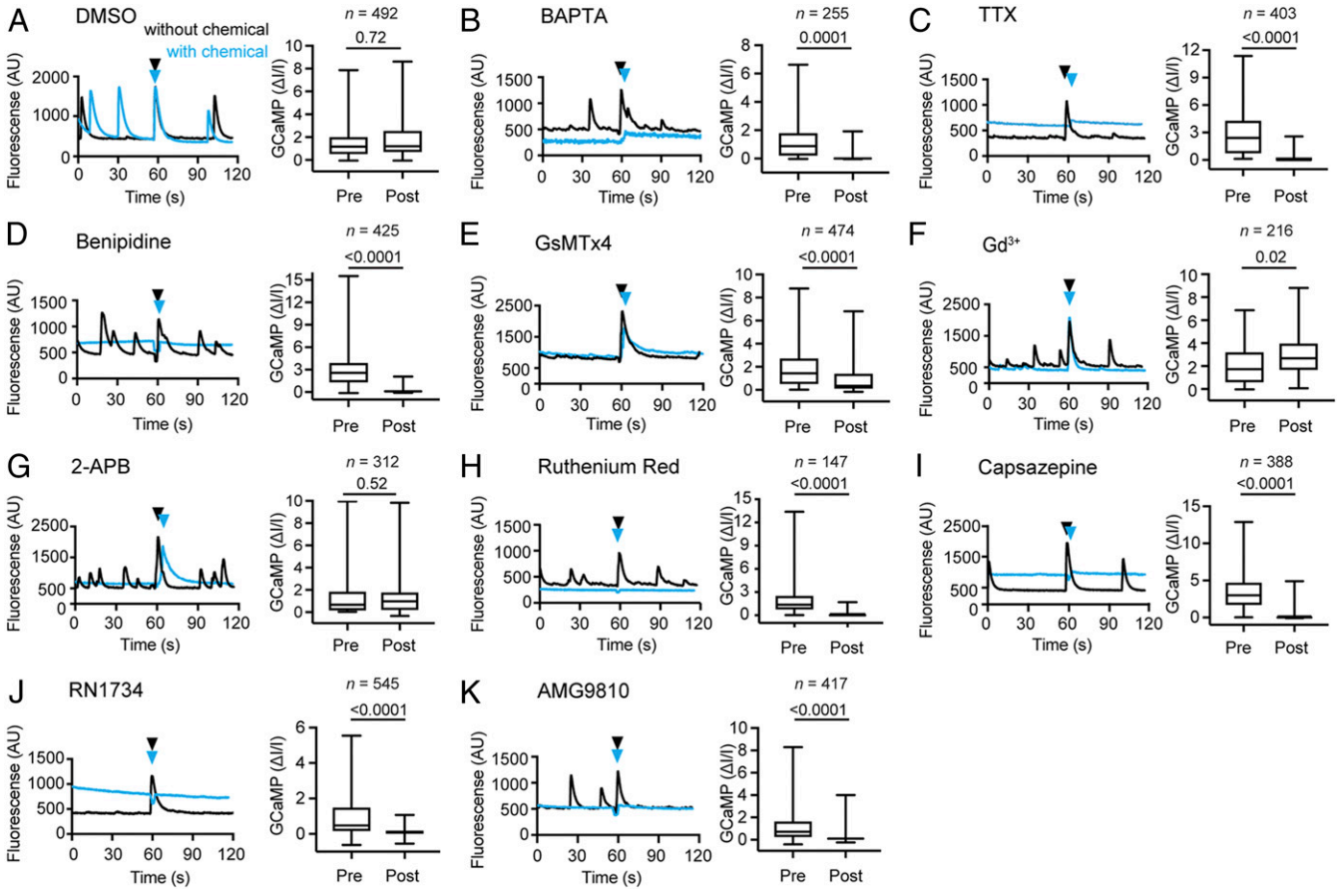

Fig. 5. TRPV and voltage-gated sodium and calcium channels contribute to mechanically evoked response to shear stress. (*A*–*K*) Averaged GCaMP6s fluorescence traces of the same set of cortical neurons mechanically stimulated by pistons before (black) and after (blue) the addition of chemical compounds to perturb channel activity. Black and blue arrowheads indicate the time of stimulation. Box and whisker plots show normalized GCaMP6s values for cortical neurons stimulated by pistons. *n* represents the number of neurons analyzed. For each box and whisker plot, data from 3 independent experiments are combined. Boxes represent mean; whiskers, minimum and maximum values. The effects of various compounds are plotted. (*A*) Vehicle alone (DMSO, 0.1% vol). (*B*) Extracellular calcium chelator BAPTA free acid (2 mM). (*C*) Voltage-gated sodium channel inhibitor TTX (1 μM). (*D*) Voltage-gated calcium channel inhibitor benipidine (1 μM). (*E*) Mechanosensitive channel inhibitor GsMTx4 (2.5 μM). (*F*) Stretch-activated channel inhibitor gadolinium chloride (Gd^{3+}; 100 μM). (*G*) Mechanosensitive channel inhibitor 2-APB (100 μM). (*H*) Nonspecific ion channel inhibitor ruthenium red (100 μM). (*I*) TRPV1/TRPV4 inhibitor capsazepine (2.5 μM). (*J*) TRPV4 inhibitor RN1734 (5 μM). (*K*) TRPV1 inhibitor AMG9810 (0.1 μM). Logistic regression was used for statistical analysis (*Materials and Methods*).

not considerably change the response to local indentations (56% vs. 66%) (*SI Appendix*, Fig. S8*C*). Application of gadolinium, a nonspecific inhibitor of stretch activated channels, increased the neuronal response to shear stress (2.0 ± 0.1 Δ*I*/*I* vs. 2.9 ± 0.1 Δ*I*/*I*) (Fig. 5*F*) but did not considerably change the response to indentation by AFM (76% vs. 74%) (*SI Appendix*, Fig. S8*D*). 2-APB, an inhibitor of TRPC1 and TRPC5 channels (32), had no considerable effect on the calcium response evoked by shear stress (1.7 ± 0.2 Δ*I*/*I* vs. 1.4 ± 0.1 Δ*I*/*I*) (Fig. 5*G*) but increased the likelihood of response (50% vs. 76%) to local indentation by AFM (*SI Appendix*, Fig. S8*F*). Ruthenium red, which inhibits a large variety of mammalian ion channels, including members of the vanilloid TRP channel family, calcium channels, ryanodine receptors, and others (33), largely inhibited the neuronal responses to shear stress by pistons (1.8 ± 0.1 Δ*I*/*I* vs. 0.2 ± 0.0 Δ*I*/*I*) (Fig. 5*H*), as well as to indentation by AFM (75% vs. 38%) (*SI Appendix*, Figs. S8*E* and S9).

We next applied capsazepine, a blocker of TRPV1 and TRPV4 channels, which strongly suppressed the neuronal response to shear stress, from 3.4 ± 0.1 Δ*I*/*I* to 0.4 ± 0.0 Δ*I*/*I* (Fig. 5*I*). Application of RN1734, a TRPV4 channel-specific blocker, inhibited the neuronal response to shear stress from 1.0 ± 0.1 Δ*I*/*I* to 0.1 ± 0.0 Δ*I*/*I* (Fig. 5*J*). Likewise, application of AMG9810, a TRPV1 channel-specific blocker, inhibited the neuronal response to shear stress from 1.1 ± 0.1 Δ*I*/*I* to 0.1 ± 0.0 Δ*I*/*I* (Fig. 5*K*). The comprehensive analysis of how all tested chemical compounds affect the neuronal response to shear stress and local indentations by AFM (*SI Appendix*, Fig. S10), suggests that the mechanically evoked response of neurons requires extracellular calcium entry and involves a variety of ion channels, primarily voltage-gated channels.

Discussion

Here we studied the response of cortical neurons to mechanical stimulation by shear stress and local indentation. We found that neurons respond differentially, either transiently with a fast decay or sustained with a slow decay, to both types of mechanical stimulation. While the response of neurons subjected to mechanical stimuli has been described previously in the context of traumatic brain injury (7, 8, 25, 26), the mechanical stimulation applied in this study does not interfere with spontaneous neuronal activity, change the cell morphology, damage the cell membrane, or alter the cytoskeletal architecture. We can exclude neuronal injury or cytoskeletal impairment resulting from mechanical stimuli. Thus, we conclude that subtraumatic forces and pressures evoke neurons to respond differentially (Fig. 6).

While shear stress predominantly evoked transient responses in neurons, the local indentation of neuronal compartments by AFM evoked both transient and sustained responses. It may be of interest to further investigate whether the mechanically induced transient response can be used to stimulate or control neuronal systems. The physiological relevance of the sustained response remains to be identified, however. While such long-lasting dysregulation of calcium is typically associated with cell death (7, 25), we found that neurons with sustained responses generally survived as long as unstimulated neurons.

In our indentation experiments, we stimulated the somas of neurons with 50 to 400 nN. These forces appear quite high; however, the relatively large contact area of the micrometer-sized beads used to mechanically stimulate neurons translates the applied force into moderate pressures ranging from 1.3 to 10.2 kPa (*SI Appendix*, Text S1). Normal intracranial pressure in a supine adult ranges from 0.9 to 2.0 kPa, while the pressure at which intensive care treatment is initiated ranges from 2.7 to 3.3 kPa (34). Similarly, the cerebrospinal fluid pressure at lumbar puncture ranges from 1.1 to 2.0 kPa when side-lying and from 2.0 to 2.9 kPa when sitting straight (34). In comparison, the predicted intracranial pressure for traumatic injury in football players is ∼90 kPa

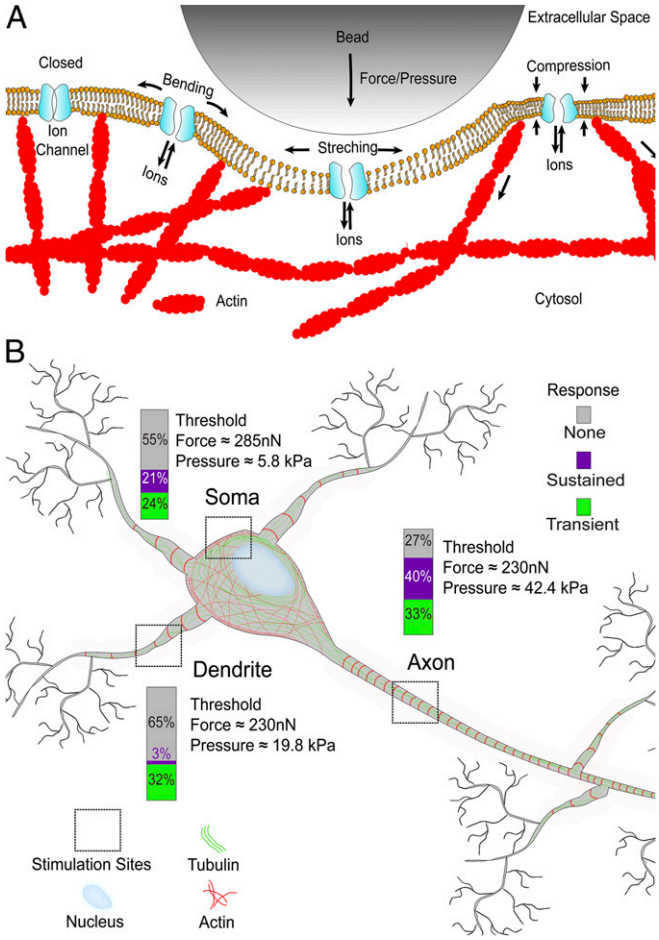

Fig. 6. Neurons differentiate the magnitude and location of mechanical stimuli. The schematic drawing summarizes the response of cortical neurons to the localized mechanical stimulation by a bead. (*A*) Our experiments support a recently suggested model (1) in which mechanical stimulation nonspecifically gates ion channels and mechanosensitive channels, which changes the voltage across the neuronal membrane and leads to calcium influx into the cytosol. (*B*) Neurons differentiate their responses to the location and magnitude of the mechanical stimulus. Gray, purple, and green parts of the bars show the percentages of neurons showing no, sustained, and transient responses to the mechanical stimulation of soma, dendrite, and axon. Average threshold forces and pressures that evoke neuronal responses are indicated for each neuronal compartment.

(35), and the intracranial pressure of mice exposed to conditions causing neural trauma is ∼100 kPa (5). Thus, the pressure applied by locally indenting a bead into the soma is slightly above normal intracranial pressure and is ∼10-fold less than the intracranial pressure causing traumatic injury. Moreover, the pressure of ∼1 to 5 Pa applied in our shear stress experiments is at least 2 orders of magnitude lower than intracranial pressure values. Although the elevated pressures applied to mechanically stimulate neurons by indenting axons or dendrites with a bead reach of 42.4 kPa and 19.8 kPa, respectively (*SI Appendix*, Text S2), they are still not in the traumatic regime. Accordingly, we did not observe any characteristic traumatic symptoms of the neurons after mechanical stimulation, suggesting that the pressures applied in our study are in the physiologically relevant, subtraumatic regime (35).

With respect to stimulus location, we found that axons show a higher probability (73%) to respond to mechanical stimulation than dendrites (35%) or somas (45%). Along with a greater probability or susceptibility to respond to mechanical stimulation, axons also show more sustained responses than transient

responses, whereas dendrites primarily respond transiently. We wondered whether the stiffness of neuronal compartments could explain the observed differences in response to mechanical stimulation and used the atomic force microscope to approximate the elastic moduli of axons, dendrites, and somas of cortical neurons (*SI Appendix*, Fig. S11) (17). In agreement with previous reports (18), we found that axons are the mechanically stiffest compartments (7.8 ± 0.8 kPa), followed by the softer dendrites (4.5 ± 0.6 kPa), and somas (0.7 ± 0.1 kPa). However, axons also have smaller diameters than dendrites (*SI Appendix*, Fig. S7 and Text S2). Thus, on exertion of an average force of ∼230 nN by the AFM cantilever, the pressure of ∼42 kPa applied to axons is significantly greater than the ∼20 kPa applied to dendrites. The greater susceptibility of axons to mechanical stimuli may be explained by the fact that the same stimulation force actually applies higher pressure to axons.

Finally, we explored how extracellular calcium enters the neurons on mechanical stimulation. To begin, we excluded the possibility of calcium entry via mechanically induced defects of the plasma membrane. Next, we investigated classical mechanosensitive channels, which appear to be obvious candidates for facilitating calcium influx (9, 19, 20). To our surprise, we found that the majority of canonical mechanosensitive channel blockers tested in our study (GsMTx4, gadolinium, and 2-APB) could not fully inhibit mechanically evoked responses. Interestingly, the TRPV channel blocker capsazepine substantially inhibited the neuronal response to mechanical stimuli. However, capsazepine also blocks voltage-gated calcium channels (36), which prompted us to test TRPV4 and TRPV1 channel-specific blockers RN1734 and AMG9810. Both compounds effectively blocked the mechanically evoked responses, suggesting that TRPV channels are involved in generating the calcium response.

TRPV1 is a multimodal calcium channel that can be activated by noxious heat (>43 °C), pH change, chemical ligands, and mechanical force (37). A recent study showed that the TRPV1 antagonist AMG9810 can inhibit responses to mechanical stimulation (38). In our study, neuronal responses to AFM stimulation are potentiated by 2-APB, a TRPV1 agonist (39), and responses to shear stress are potentiated by gadolinium, which sensitizes TRPV1 (40). These perturbation experiments suggest an involvement of TRPV class receptors in our observed neuronal responses. Importantly, however, application of a voltage-gated sodium channel blocker (TTX), a voltage-gated calcium channel blocker (benipidine), and a generic ion channel blocker (ruthenium red) also suppressed the mechanically evoked response of cortical neurons. These findings suggest that the voltage-gated channels either directly allow passage of calcium through the neuronal membrane or indirectly lead to secondary calcium flux by depolarization of the membrane.

In summary, our data are in excellent agreement with previous studies establishing that a number of neuronal ion channels not conventionally described as mechanosensitive channels, including NMDA receptors (41), voltage-gated potassium channels (42) and voltage-gated sodium channels (43), can be mechanically modulated. The resulting model proposed by Tyler (1) describes how neurons may open ion channels nonspecifically in response to force and/or pressure acting on the membrane protein, plasma membrane, cytoskeleton, and/or extracellular matrix. Here we extend this model by demonstrating that the neuronal compartments soma, dendrite, and axon respond differentially to mechanical stimulation and providing the pressure/force values at which each compartment prefers to respond in a transient or/and sustained manner (Fig. 6).

Taken together, our findings provide a quantitative and morphological framework to mechanically stimulate neurons. We show that cortical neurons respond to both globally and locally applied mechanical forces and pressures by calcium influx through ion channels. The type of the neuronal response, whether transient or sustained, is differentiated by the magnitude and location of the mechanical stimulus. Thus, our insights are useful for understanding how neurons respond to mechanical cues in vitro. Since neuronal responses to mechanical stimuli are highly dependent on the in vitro and in vivo context, we cannot project our findings to multicellular and organismal levels. However, electrophysiology studies in brain slices (9) and ultrasound-mediated neuromodulation in vitro and in vivo (10, 11) suggest that the mechanosensitivity of neuronal responses is an universal phenomenon with relevance across a range of species and experimental settings. Thus, our insight into how mechanical stimuli may be applied to guide the differential response of neurons may lead to novel applications to control ion channels and neuronal systems.

Materials and Methods

Neuron Culture. Neurons were cultured following a standard protocol. First, 50,000 cells were seeded onto the coverslip and allowed to attach for 30 min, followed by the addition of 1 mL of neurobasal medium. Cultures were maintained inside an incubator under controlled environmental conditions (37 °C and 5% CO_2), and one-half of the neurobasal medium supplemented with 0.5 mM GlutaMAX and 2% B27 (Thermo Fisher Scientific) was exchanged every 3 d.

Combined Shear Stress and Widefield Microscopy. A 96-piston array was 3D-printed by Protolabs using ABS black resin (SL7820; 3D Systems). Each piston had a circular face with a diameter of 5.4 mm. The piston array was attached to a loudspeaker (W3-1750S; TB Speakers) that actuated the piston array vertically. A signal generator (DS345; Stanford Research Systems) was used to generate a low-frequency (60 Hz) sign wave, which was amplified with an amplifier (SPL400; Skytec). This amplified signal was used to drive the speaker and actuate the piston array. The piston device was mounted on a widefield microscope (Nikon Eclipse Ti) equipped with a 10× air objective (Nikon Plan Fluor 10×/0.3), an illumination system (Spectra X7; Lumencor), and an environmental chamber for CO_2 and temperature control. Time-lapse images were acquired with 488-nm excitation and 100-ms exposure. Following published procedures (15, 44), we estimated the pressure applied in our shear stress experiments to range from ∼1 to 5 Pa.

Combined AFM and Confocal Microscopy. In brief, confocal imaging was performed using an inverted laser-scanning confocal microscope (Observer Z1, LSM 700; Zeiss) equipped with a 25×/0.8 LCI PlanApo water immersion objective (Zeiss). An atomic force microscope (CellHesion 200; JPK Instruments) was mounted onto the confocal microscope. Mechanical stimulation protocols were programmed using the JPK CellHesion software.

Functional Calcium Imaging. Genetically encoded calcium sensors were expressed in neurons using adeno-associated viruses. AAV1 -EF1a-GCaMP6S-(1.8×10^{13} vg mL^{-1}) and EF1a-GCaMP6F (6.1×10^{11} vg mL^{-1}) were used at a multiplicity of infection of 5.0×10^4 to express GCaMP6S and GCaMP6F, respectively. Neurons were infected at 2 to 6 d in vitro (DIV), expression was usually seen at 5 to 9 DIV, and experiments were performed at 10 to 30 DIV unless noted otherwise. If the GCaMP6S fluorescence signal of a mechanically stimulated neuron increased by a factor of ≥0.1 (e.g., ≥10%) it was counted as response for both the analysis of piston and AFM experiments.

Live Cell Staining. To identify axons for subcellular stimulation, we stained neurons using an anti–pan-neurofascin primary antibody (clone A12/18; NeuroMab) that labels the axon initial segment, followed by a secondary Alexa Fluor 594–F(ab′)2–anti-mouse antibody (Invitrogen). In brief, neurons were washed once with neurobasal medium and then incubated with 400 μL of anti–pan-neurofascin antibody at 1:100 dilution in neurobasal medium for 5 min at 37 °C in the incubator. Neurons were washed 3 times with warm neurobasal medium and then incubated with 500 μL of secondary antibody at 1:500 dilution for 40 s at room temperature with gentle agitation. Neurons were rinsed 3 times with neurobasal medium and then returned to the incubator for >30 min before starting the experiment.

Chemical Reagents. Chemical inhibitors were obtained from Enzo Life Sciences, Sigma-Aldrich, or Tocris. Concentrations and application procedures for chemical inhibitors are provided in *SI Appendix, Materials and Methods*.

Functional Calcium Imaging Analysis. For AFM recordings, an average calcium signal curve, $\Delta I/I$, was calculated as the mean signal over the entire image relative to the first time point of the curve using a custom MATLAB code. For piston experiments, cells were identified, and their fluorescence was plotted over time. Normalized GCaMP fluorescence values, $\Delta I/I$, were calculated for each cell using $\Delta I/I = (I_{max} - I_{ave})/I_{ave}$, where I_{max} is the peak fluorescence intensity value at t_{max} and I_{ave} is the average fluorescence intensity value preceding the stimulation. We further calculated the decay times and classified responses as transient if they were <2.8 s and as sustained if they were >2.8 s. Further details on peak value determination, thresholding, and time frames for analysis are provided in *SI Appendix, Materials and Methods*.

Superresolution Microscopy. STED microscopy was performed using a STEDYCON head (Abberior Instruments) mounted onto a BX53 microscope body (Olympus) and equipped with a UPlanSApo 100×/1.4 oil objective (Olympus). Neurons were fixed and stained, first with anti–pan-neurofascin primary antibody (clone A12/18; NeuroMab) at 1:100 dilution and then with secondary Alexa Fluor 594–F(ab′)2–anti-mouse antibody (Invitrogen) at 1:200 dilution and with phalloidin-STAR RED (Abberior Instruments) at a concentration of 1 unit mL^{-1} for 1 h at room temperature.

Statistical Analysis. Statistical analysis was performed using GraphPad Prism 7 and custom-made MATLAB scripts. The nonparametric 2-tailed Mann–Whitney *U* test, nonparametric 1-way ANOVA (Kruskal–Wallis test), χ^2 test for goodness of fit, and logistic regression relating treatment and time points to the variable $\Delta I/I$ were used for statistical analysis.

Data Availability Statement. The data supporting the findings of this study are available from the corresponding author on reasonable request.

Code Availability Statement. Custom MATLAB code written for the calcium imaging data analysis are available from the corresponding authors on reasonable request.

ACKNOWLEDGMENTS. We thank N. Strohmeyer, C. Cattin, J. Helenius, G. Flaeschner, and D. Martinez-Martin for constructive ideas and discussion; B. M. Lang for help with statistical analysis; Abberior Instruments for providing the STED microscope and J. Hanne for excellent support; A. Ponti for help with image analysis of shear stress experiments; J. Jüttner and C. P. Partino Alvarez for help with AAV production; and S. Ronchi and J. Bartram for with neuron preparation. The work was supported by a long-term European Molecular Biology Organization (EMBO) fellowship (ALTF 424-2016, to B.M.G.), an Eidgenössische Technische Hochschule Zurich grant (ETH-28 16-2), and the National Center of Competence in Research, Molecular Systems Engineering.

1. W. J. Tyler, The mechanobiology of brain function. *Nat. Rev. Neurosci.* **13**, 867–878 (2012).
2. C. E. Morris, Voltage-gated channel mechanosensitivity: Fact or friction? *Front. Physiol.* **2**, 25 (2011).
3. B. Pan *et al*., TMC1 forms the pore of mechanosensory transduction channels in vertebrate inner ear hair cells. *Neuron* **99**, 736–753.e6 (2018).
4. M. Chalfie, Neurosensory mechanotransduction. *Nat. Rev. Mol. Cell Biol.* **10**, 44–52 (2009).
5. L. E. Goldstein *et al*., Chronic traumatic encephalopathy in blast-exposed military veterans and a blast neurotrauma mouse model. *Sci. Transl. Med.* **4**, 134ra60 (2012).
6. J. Mez *et al*., Clinicopathological evaluation of chronic traumatic encephalopathy in players of American football. *JAMA* **318**, 360–370 (2017).
7. D. Kilinc, G. Gallo, K. A. Barbee, Mechanically-induced membrane poration causes axonal beading and localized cytoskeletal damage. *Exp. Neurol.* **212**, 422–430 (2008).
8. V. E. Johnson, W. Stewart, D. H. Smith, Axonal pathology in traumatic brain injury. *Exp. Neurol.* **246**, 35–43 (2013).
9. Y. A. Nikolaev, P. J. Dosen, D. R. Laver, D. F. van Helden, O. P. Hamill, Single mechanically-gated cation channel currents can trigger action potentials in neocortical and hippocampal pyramidal neurons. *Brain Res.* **1608**, 1–13 (2015).
10. Y. Tufail *et al*., Transcranial pulsed ultrasound stimulates intact brain circuits. *Neuron* **66**, 681–694 (2010).
11. W. Lee *et al*., Image-guided transcranial focused ultrasound stimulates human primary somatosensory cortex. *Sci. Rep.* **5**, 8743 (2015).
12. W. Lee *et al*., Transcranial focused ultrasound stimulation of human primary visual cortex. *Sci. Rep.* **6**, 34026 (2016).
13. H. Guo *et al*., Ultrasound produces extensive brain activation via a cochlear pathway. *Neuron* **98**, 1020–1030.e4 (2018). Correction in: *Neuron* **99**, 866 (2018).
14. T. Sato, M. G. Shapiro, D. Y. Tsao, Ultrasonic neuromodulation causes widespread cortical activation via an indirect auditory mechanism. *Neuron* **98**, 1031–1041.e5 (2018).
15. J. Xu *et al*., GPR68 senses flow and is essential for vascular physiology. *Cell* **173**, 762–775.e16 (2018).
16. D. Alsteens *et al*., Atomic force microscopy-based characterization and design of biointerfaces. *Nat. Rev. Mater.* **2**, 17008 (2017).
17. M. Krieg *et al*., Atomic force microscopy-based mechanobiology. *Nat. Rev. Phys.* **1**, 41–57 (2019).
18. Y. Zhang *et al*., Modeling of the axon membrane skeleton structure and implications for its mechanical properties. *PLoS Comput. Biol.* **13**, e1005407 (2017).
19. D. E. Koser *et al*., Mechanosensing is critical for axon growth in the developing brain. *Nat. Neurosci.* **19**, 1592–1598 (2016).
20. K. Franze *et al*., Neurite branch retraction is caused by a threshold-dependent mechanical impact. *Biophys. J.* **97**, 1883–1890 (2009).
21. S. P. Ramanathan *et al*., Cdk1-dependent mitotic enrichment of cortical myosin II promotes cell rounding against confinement. *Nat. Cell Biol.* **17**, 148–159 (2015).
22. M. P. Stewart *et al*., Hydrostatic pressure and the actomyosin cortex drive mitotic cell rounding. *Nature* **469**, 226–230 (2011).
23. Y. Toyoda *et al*., Genome-scale single-cell mechanical phenotyping reveals disease-related genes involved in mitotic rounding. *Nat. Commun.* **8**, 1266 (2017).
24. C. Leterrier *et al*., Ankyrin G membrane partners drive the establishment and maintenance of the axon initial segment. *Front. Cell. Neurosci.* **11**, 6 (2017).
25. D. M. Geddes, R. S. Cargill, 2nd, An in vitro model of neural trauma: Device characterization and calcium response to mechanical stretch. *J. Biomech. Eng.* **123**, 247–255 (2001).
26. D. M. Geddes, R. S. Cargill, 2nd, M. C. LaPlaca, Mechanical stretch to neurons results in a strain rate- and magnitude-dependent increase in plasma membrane permeability. *J. Neurotrauma* **20**, 1039–1049 (2003).
27. E. D'Este, D. Kamin, F. Göttfert, A. El-Hady, S. W. Hell, STED nanoscopy reveals the ubiquity of subcortical cytoskeleton periodicity in living neurons. *Cell Rep.* **10**, 1246–1251 (2015).
28. K. Xu, G. Zhong, X. Zhuang, Actin, spectrin, and associated proteins form a periodic cytoskeletal structure in axons. *Science* **339**, 452–456 (2013).
29. P. R. Williams *et al*., A recoverable state of axon injury persists for hours after spinal cord contusion in vivo. *Nat. Commun.* **5**, 5683 (2014).
30. M. M. Moran, H. Xu, D. E. Clapham, TRP ion channels in the nervous system. *Curr. Opin. Neurobiol.* **14**, 362–369 (2004).
31. P. A. Gottlieb, F. Sachs, Piezo1: Properties of a cation selective mechanical channel. *Channels (Austin)* **6**, 214–219 (2012).
32. C. Strübing, G. Krapivinsky, L. Krapivinsky, D. E. Clapham, TRPC1 and TRPC5 form a novel cation channel in mammalian brain. *Neuron* **29**, 645–655 (2001).
33. R. Tapia, I. Velasco, Ruthenium red as a tool to study calcium channels, neuronal death and the function of neural pathways. *Neurochem. Int.* **30**, 137–147 (1997).
34. L. A. Steiner, P. J. Andrews, Monitoring the injured brain: ICP and CBF. *Br. J. Anaesth.* **97**, 26–38 (2006).
35. L. Zhang, K. H. Yang, A. I. King, A proposed injury threshold for mild traumatic brain injury. *J. Biomech. Eng.* **126**, 226–236 (2004).
36. R. J. Docherty, J. C. Yeats, A. S. Piper, Capsazepine block of voltage-activated calcium channels in adult rat dorsal root ganglion neurones in culture. *Br. J. Pharmacol.* **121**, 1461–1467 (1997).
37. S. Sawamura, H. Shirakawa, T. Nakagawa, Y. Mori, S. Kaneko, "TRP channels in the brain: What are they there for?" in *Neurobiology of TRP Channels*, T. L. R. Emir, Ed. (Boca Raton, FL, ed. 2, 2017), pp. 295–322.
38. N. R. Gavva *et al*., AMG 9810 [(E)-3-(4-t-butylphenyl)-N-(2,3-dihydrobenzo[b][1,4]dioxin-6-yl)acrylamide], a novel vanilloid receptor 1 (TRPV1) antagonist with antihyperalgesic properties. *J. Pharmacol. Exp. Ther.* **313**, 474–484 (2005).
39. C. K. Colton, M. X. Zhu, 2-Aminoethoxydiphenyl borate as a common activator of TRPV1, TRPV2, and TRPV3 channels. *Handb. Exp. Pharmacol.* **179**, 173–187 (2007).
40. K. Tousova, L. Vyklicky, K. Susankova, J. Benedikt, V. Vlachova, Gadolinium activates and sensitizes the vanilloid receptor TRPV1 through the external protonation sites. *Mol. Cell. Neurosci.* **30**, 207–217 (2005).
41. P. Paoletti, P. Ascher, Mechanosensitivity of NMDA receptors in cultured mouse central neurons. *Neuron* **13**, 645–655 (1994).
42. I. V. Tabarean, C. E. Morris, Membrane stretch accelerates activation and slow inactivation in Shaker channels with S3-S4 linker deletions. *Biophys. J.* **82**, 2982–2994 (2002).
43. J. A. Wolf, P. K. Stys, T. Lusardi, D. Meaney, D. H. Smith, Traumatic axonal injury induces calcium influx modulated by tetrodotoxin-sensitive sodium channels. *J. Neurosci.* **21**, 1923–1930 (2001).
44. S. S. Ranade *et al*., Piezo1, a mechanically activated ion channel, is required for vascular development in mice. *Proc. Natl. Acad. Sci. U.S.A.* **111**, 10347–10352 (2014).